PHYSICAL REVIEW E **91**, 012122 (2015)

Dynamics of a rigid rod in a disordered medium with long-range spatial correlation

M. Ebrahim Foulaadvand[1,2,*] and Mahdiyeh Sadrara[3]

[1]*Department of Physics, University of Zanjan, P.O. Box 45196-313, Zanjan, Iran*

[2]*School of Nano-science, Institute for Research in Fundamental Sciences (IPM), P.O. Box 19395-5531, Tehran, Iran*

[3]*Department of Physics, Kharazmi University, P.O. Box 15614, Tehran, Iran*

(Received 1 April 2013; revised manuscript received 24 November 2014; published 12 January 2015)

We investigate the diffusion of a rigid rodlike object in a two-dimensional disordered host medium, which consists of static pointlike sources of force. The points are distributed with long-range spatial correlation and interact with the rod via a repulsive potential. The time dependence of the rod's center-of-mass mean-squared displacement and its rotational mean-squared displacement are obtained for various degrees of long-range spatial correlation and rod's lengths. These transport characteristics are compared to those obtained in previous studies for the case of homogeneous distribution of force points. It is shown that existence of long-range correlation among force points makes the center of mass diffusion anomalous.

DOI: 10.1103/PhysRevE.91.012122 PACS number(s): 05.40.−a, 66.30.−h

I. INTRODUCTION

Transport processes in disordered media constitute an important class of problems especially in the light of their relevance to the modeling of a vast variety of phenomena in physics and many interdisciplinary areas. A partial list of applications include transport phenomena in porous media, diffusion in biological tissues, and conduction through composite solids [1–5]. It is a well-established fact the characteristics of disorder can strongly affect the transport properties of equilibrium as well as out-of-equilibrium systems. In particular, Lorentz gas [6,7] has served as a simple model describing the transport of a single particle in a disordered medium. In a Lorentz gas, a single classical particle moves through a disordered array of static objects. Lorentz gas can generally be used for modeling the motion of light particles in a disordered environment. When the density of static objects in the host medium increases, the dynamics of the diffusive particle becomes complicated and the system exhibits the typical aspects of the dynamics of supercooled liquids and dense colloidal systems [8,9]. Obstacles and diffusive particles are normally assumed as spheres and disks. Recently considerable attention has been paid to the case where the shape of the diffusive particle deviates from sphere and is endowed with rotational degrees of freedom [10,11]. Especially, rodlike objects have been notably explored [12–18]. In Refs. [19–21], the characteristics of a generalization of Lorentz gas in which the diffusive particle is a rigid rodlike particle has been deeply investigated. Analogous to supercooled liquids [22–26] and dense colloidal systems [27–29], it was observed that at intermediate times, the rod center of mass (CM) exhibits a caging regime, which is due to steric hindrance emerging from neighboring obstacles. Additionally, diffusion of rodlike objects in disordered media is directly related to experiment. For instance, suspension of semiflexible polymers have been shown to exhibit a variety of dynamical phenomena of great importance to both physics and biology that are still only poorly understood. For high concentration, the polymeric suspension undergoes a phase transition to a nematic phase with long-range orientational order. Recently the self-diffusion of rodlike viruses in the anisotropic nematic phase has been experimentally explored [30]. The diffusion of colloidal rods has been empirically studied by the technique of fluorescence recovery after photo bleaching [31]. Motivated by the above arguments, we believe that investigation of Lorentz gas properties in disordered media could shed more light onto the problem. In many situations, the disordered media can support some degrees of correlations especially long-range ones [32,33]. Therefore it would be a natural question to what extent the diffusion characteristics are affected by spatial correlations [34]. In this paper we aim to investigate the properties of the Lorentz gas in a force medium with spatially correlated distribution of obstacles.

II. MODEL DESCRIPTION AND ITS FORMULATION

Our diffusive particle is supposed to have a rodlike shape. Moreover, we assume this particle, hereafter called a rod, is rigid. The rod is modeled by a set of N aligned beads with distance 2σ between each other. The rod length is hence $L_{\rm rod} = (2N-1)\sigma$. The rod mass is mN where m is the mass of each constituent bead. The rod performs a classical motion in a host medium where for simplicity and reducing the simulation costs is assumed to be two dimensional. The medium consists of static pointlike sources of force called obstacles, each of which interact with any of the rod beads via a soft-disk potential. Analogous to [19–21], we assume the potential takes a short-ranged repulsive form $V(r) = \epsilon(\frac{\sigma}{r})^{12}$. We exclude the attractive part of the Lennard-Jones potential to avoid the possibility of rod trapping by the obstacles. The medium is characterized by the statistical properties of the obstacles spatial distribution. We define the number density of obstacles as $\rho = \frac{N_{\rm obs}}{L^2}$ in which L is the size of the $2d$ simulation box and $N_{\rm obs}$ denotes the number of obstacles. In a series of papers, Moreno and Kob have thoroughly investigated the relaxation dynamics of the rod by studying its center-of-mass translational and rotational degrees of freedom [19–21]. In their investigations they considered both an inhomogeneous random distribution of obstacles and a more ordered one in which the distribution of obstacles has a homogeneous glassy structure. Notable difference were observed for these two types of structure. In this paper, we aim to study the influence of

*foolad@iasbs.ac.ir

long-range spatial correlation in the host medium on the rod's relaxation dynamics. In order to construct spatially correlated obstacles, we exploit the fractional Brownian motion (fBm). Consider a one-dimensional random process in which the stochastic field h depends on the independent variable x. This process is called a fBm with Hurst exponent $0 < H < 1$ if the following condition holds [3]:

$$\langle [h(x_1) - h(x_2)]^2 \rangle \propto (x_1 - x_2)^{2H}, \tag{1}$$

where the average $\langle\rangle$ is over an ensemble of different realisations of the stochastic field $h(x)$. A typical example includes the random surface growth where the stochastic field $h(x)$ represents the height of stochastic surface at point x. When the exponent H is between zero and unity, we say that the field h acquires long-range spatial correlation. The fBm is divided into three distinctive categories. $H < \frac{1}{2}$, $H = \frac{1}{2}$ and $H > \frac{1}{2}$. If $0 < H < 0.5$ the fBm is anti correlated (negative correlation). $H = 0.5$ characterizes an uncorrelated fBm and $0.5 < H < 1$ corresponds to a correlated (long-range correlation) fBm. The classification holds in higher-dimensional fBm. In general for a d-dimensional fBM we have:

$$\langle [h(\mathbf{x}_1) - h(\mathbf{x}_2)]^2 \rangle \propto |\mathbf{x}_1 - \mathbf{x}_2|^{2H}. \tag{2}$$

Taking the independent variable to be time and the stochastic field h to be the distance x of a random walker to the origin the notion of fBM can be applied to random walks as well. This gives us the long time scaling behavior of a random walker, i.e., $\langle [x(t_1) - x(t_2)]^2 \rangle \sim (t_1 - t_2)^{2H}$. Note the case $H = 0.5$ corresponds to the normal diffusion. There exists a variety of methods for generation of fBM in the literature [1,35]. Midpoint, independent jumps, displacing interpolated points and Fourier filtering are a few ones. In this paper, we have implemented the Fourier method. We now explain the construction method for a static force medium with long-range correlation. Given the obstacles number density ρ and the Hurst exponent H, we first specify the simulation box size L. Then we generate $N_{\text{obs}} = \rho L^2$ correlated random numbers $\tilde{x}_1, \tilde{x}_2, \ldots, \tilde{x}_{N_{\text{obs}}}$ from our code. In general, these numbers will not be confined to the simulation box and we must apply two sets of transformations on them. Denoting their minimum and maximum by $\tilde{x}_{\min}$ and $\tilde{x}_{\max}$ the first set of transformations will be a shift that is $\tilde{x}_i^{(1)} = \tilde{x}_i - \tilde{x}_{\min}$, $i = 1,2,\ldots,N_{\text{obs}}$. After applying this transformation all $\tilde{x}_i^{(1)}$ will be positive. The second transformation is a dilation, which brings all the points into the simulation box: $\tilde{x}_i^{(2)} = \frac{\tilde{x}_i^{(1)}}{\tilde{x}_{\max} - \tilde{x}_{\min}}$, $i = 1,2,\ldots,N_{\text{obs}}$. The long-range variables $\tilde{x}_i^{(2)}$ can now be considered as the x_i coordinates of the obstacle points. In a similar manner, the y_i coordinates of the obstacles points are generated. Figure 1 exhibits two samples of obstacles generated by fBm process. We remark that there is no cross correlation between x and y coordinates of the obstacle points.

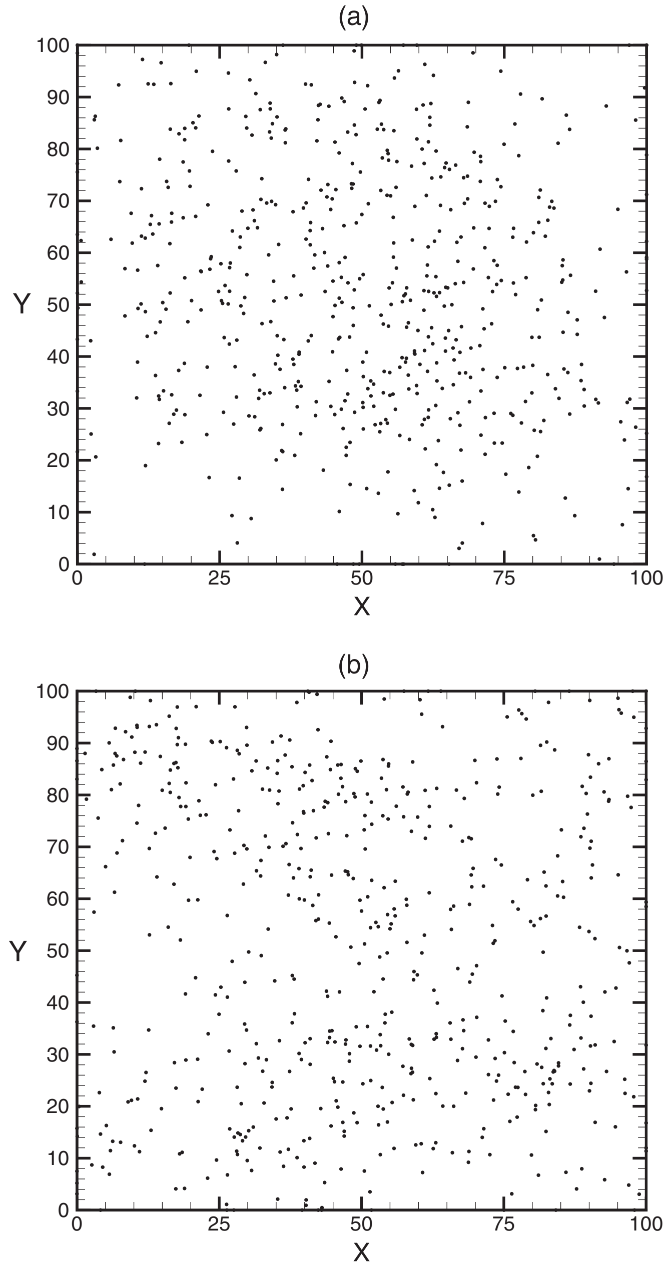

FIG. 1. (a) A sample of anticorrelated distribution of obstacles with Hurst exponent $H = 0.2$. (b) A correlated sample with $H = 0.7$. In both figures the number density is $\rho = 0.06$.

III. SIMULATION RESULTS

We now report our molecular dynamics simulation results. Prior to that, let us define the quantities by which we wish to characterize the statistical properties of the rod's motion. The rod center-of-mass (CM) mean-squared displacement $\langle [\Delta r(t)]^2 \rangle$ and its orientational mean-squared displacement $\langle [\Delta\phi(t)]^2 \rangle$ are basic quantities to describe the statistical features of the rod's movement. Space and time are measured in units σ and $\sigma(m/\epsilon)^{\frac{1}{2}}$ respectively. For each ρ, the average distance between obstacles turns out to be $\langle d \rangle \propto \rho^{-\frac{1}{2}}$. All averages were performed over 100 samples of obstacles and for each sample we have averaged over 200 different initial conditions of the rod. The length of simulation box has been $L = 800$. In each initialization, a single rod starts its motion with a constant total energy E in reduced units. We have taken the total energy of rod equal to one unless otherwise stated. The CM of each rod is randomly set within a box of size $\frac{L}{10}$ centered in the middle of the simulation box. Its orientation

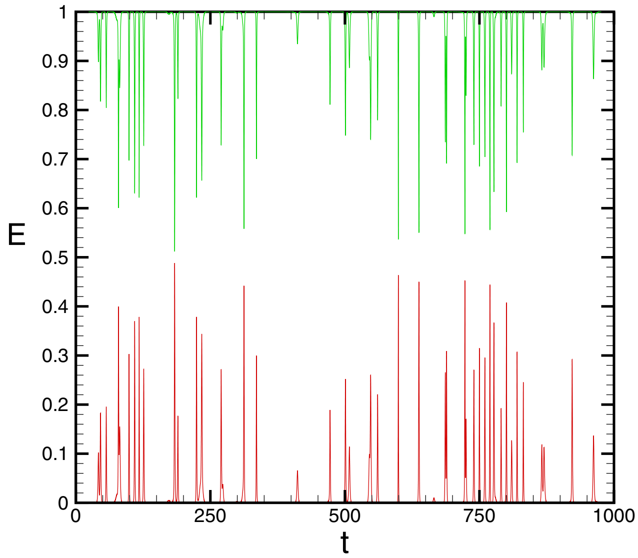

FIG. 2. (Color online) Time series of rod's kinetic (top) and potential (bottom) energies. The rod's length is $L_{\rm rod} = 29$ and its total energy is $E = 1$. The medium is characterized with $H = 0.2$ and $\rho = 0.006$.

is randomly chosen between 0 and 2π. The initialization is accepted provided the distance between each rod's bead to any of the force points is larger than σ. If this criteria is not fulfilled another attempt takes place. Furthermore, we have set the initial angular velocity in a manner that half of the kinetic energy is rotational. The direction of CM velocity is randomly chosen between $[0,2\pi]$ and its x and y components are taken equal to each other. Once the rod's CM exits the simulation box the run terminates. Before discussing the behavior of $\langle[\Delta r(t)]^2\rangle$ and $\langle[\Delta\phi(t)]^2\rangle$ let us look at the time series of the rod kinetic energy E_K and its potential energy E_P in Fig. 2 for a typical run. Note that the total energy satisfies $E = E_k + E_p$. The medium is characterized by $H = 0.2$ and $\rho = 0.006$.

As can be seen, most of the energy is in the form of kinetic and only a tiny portion is devoted to the potential part. This behavior is generic for other values of $H, \rho, L_{\rm rod}$ and total energy E. In terms of molecular dynamics terminology, we have performed all our simulations in NEV ensemble. In this ensemble, the temperature can be defined via the relation $\langle E_k\rangle = k_B T$. In our subsequent simulations, we have chosen $E = 1$, which corresponds to $k_B T \simeq 1$.

A. Diffusion in a medium with $H < 0.5$

Now let us discuss the temporal dependence of translational and angular MSDs. Figure 3 exhibits the dependence of $\langle[\Delta\phi(t)]^2\rangle/t$ and $\langle[\Delta r(t)]^2\rangle/t$ on time t for an anticorrelated distribution of obstacles characterized by the Hurst exponents $H = 0.2$ in a medium with $\rho = 0.006$.

For both displacements, one can distinguish between two different regimes. In the first regime, $\langle[\Delta r(t)]^2\rangle$ and $\langle[\Delta\phi(t)]^2\rangle$ exhibit quadratic dependence on time. This is a signature of directed motion in which the diffusion plays no dominant role. After a certain time, the rod's motion undergoes substantial changes. Let us first discuss the angular motion. As you can see

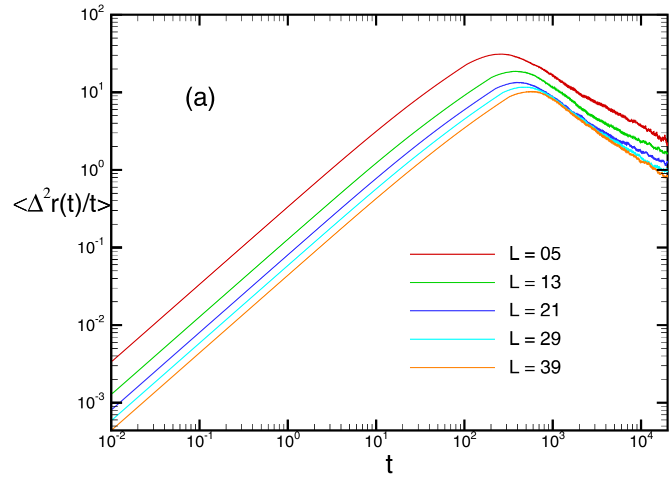

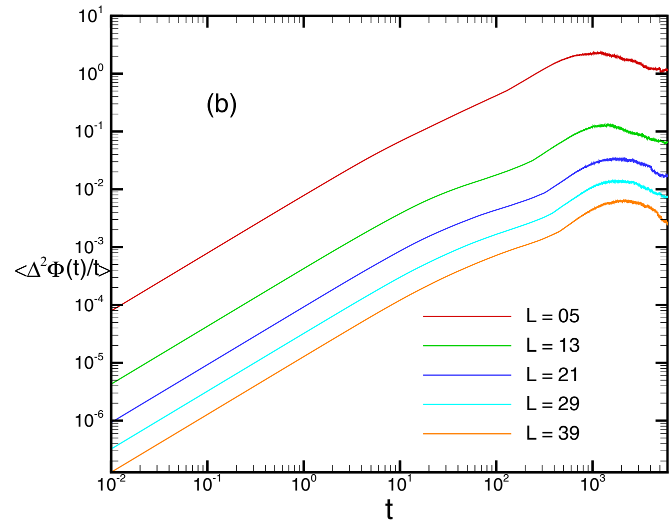

FIG. 3. (Color online) (a) Positional mean-squared displacement and (b) angular mean-squared displacement of CM in a medium with Hurst exponent $H = 0.2$ and $\rho = 0.006$ for various $L_{\rm rod}$.

from Fig. 3, the directed angular motion of the rod smoothly terminates and $\langle[\Delta\phi(t)]^2\rangle$ exhibits a linear dependence on time. It turns out that angular motion is diffusive. The diffusion constant of the corresponding random angular motion is a decreasing function of the rod length $L_{\rm rod}$. This seems natural because larger rods are more entangled among the obstacles. Let us consider the translational motion of CM. Analogous to angular motion, the results shown in Fig. 3 depict that the directed motion of CM terminates after a transition time beyond which the CM motion exhibits diffusive behavior. The significant point is that the diffusive motion of CM is not normal but anomalous. We recall that in the case of uncorrelated distribution of obstacles with the same number density, rod's CM shows a normal diffusion after termination of its directed motion [19,22]. The reason we observe anomalous diffusion is entirely due to the existence of long-range correlation among the obstacles. As a matter of fact, anticorrelation crucially changes the nature of the CM's diffusion to a subdiffusive one with scaling exponent $\delta < 1$,

$$\langle[\Delta r(t)]^2\rangle = Dt^{\delta}. \tag{3}$$

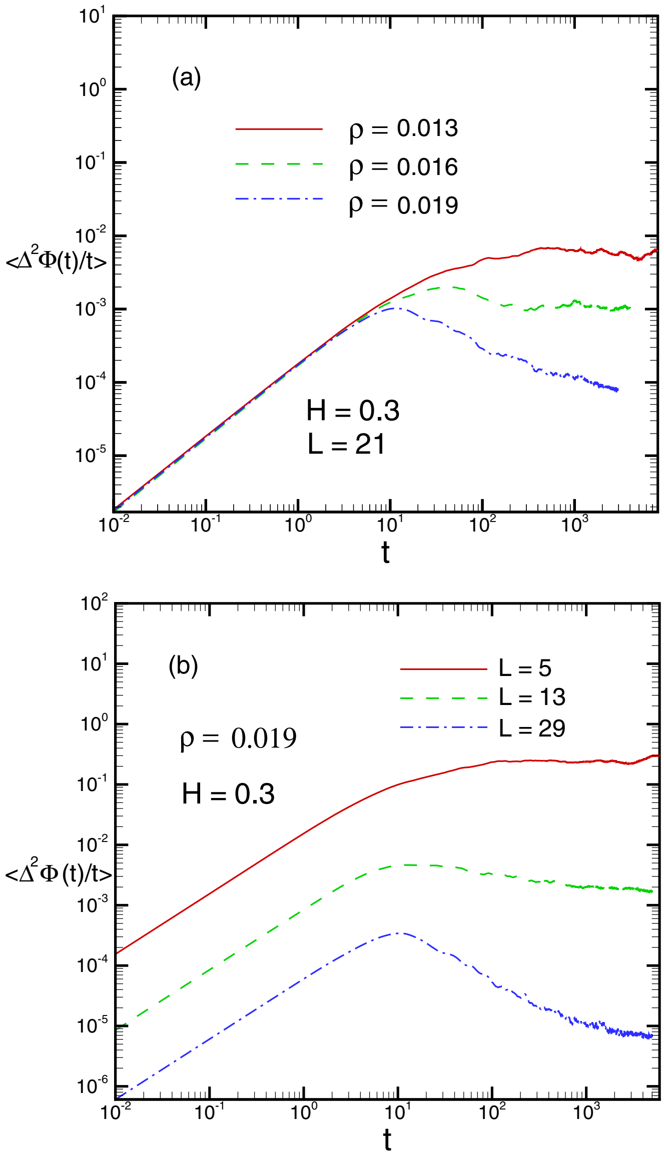

FIG. 4. (Color online) (a) Angular mean-squared displacement for a rod of length $L = 21$ in a correlated medium with $H = 0.3$ for various densities. (b) Angular mean-squared displacement in a dense medium characterized by density $\rho = 0.019$ and the Hurst exponent $H = 0.3$ for various rod's length.

We have obtained the values of exponent δ for different rod lengths L_{rod}. The length of the rod is varied from $L = 5$ to $L = 39$ and the corresponding scaling exponent δ turned out to be $0.48 \pm 0.039, 0.45 \pm 0.041.0.40 \pm 0.048, 0.38 \pm 0.051$, and 0.34 ± 0.029. It demonstrates the strong effect of anticorrelation in comparison with normal value $\delta = 1$. Rotational motion, in contrast to translational one, does not show anomalous behavior and after some transient time asymptotically tends to a normal diffusion. Nevertheless, if we increase the density or the rod's length, the subdiffusive behavior will also be observed the rotational degree of freedom. Figure 4 shows the temporal dependence of angular motion MSD for a denser medium.

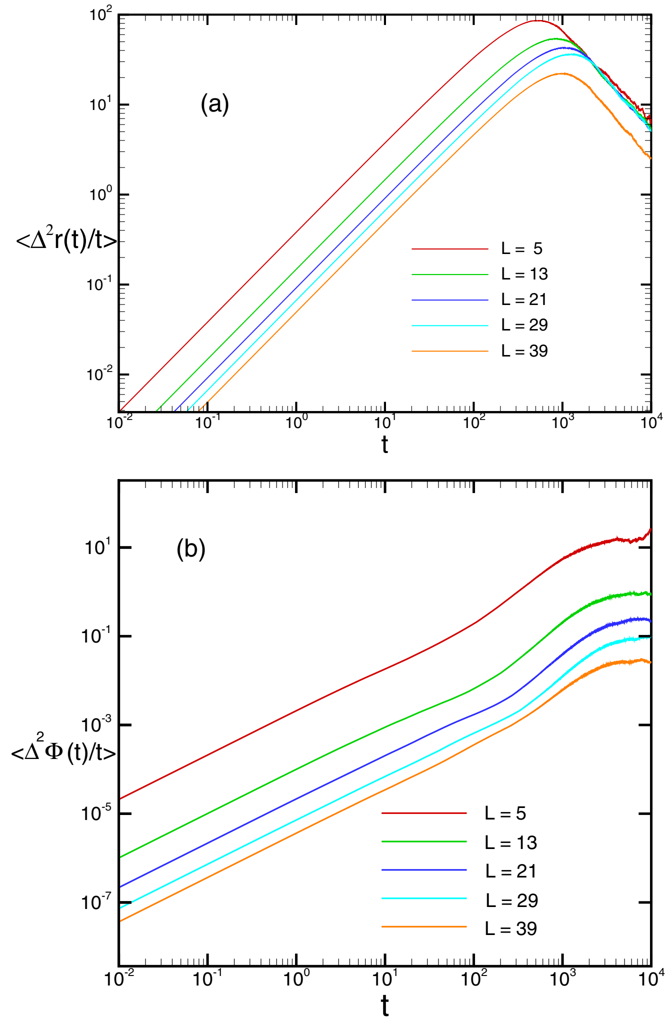

FIG. 5. (Color online) (a) Mean-squared displacement of CM, and (b) angular mean-squared displacement in a medium characterized by the Hurst exponent $H = 0.7$ and $\rho = 0.006$.

B. Diffusion in a medium with $H > 0.5$

In Fig. 5, we exhibit the time dependence of $\langle[\Delta r(t)]^2\rangle$ and $\langle[\Delta\phi(t)]^2\rangle$ for the same density $\rho = 0.006$ but in a force medium with $H = 0.7$ having long-range correlation. The generic behavior of $\langle[\Delta r(t)]^2\rangle$ is analogous to the anticorrelated case of $H = 0.2$. One observes the anomalous diffusion. Nevertheless, there is a distinguishing effect between $H = 0.2$ and $H = 0.7$. The scaling exponent δ is noticeably lower in the correlated situation $H = 0.7$. The scaling exponents are $0.21 \pm 0.016, 0.18 \pm 0.019, 0.16 \pm 0.023$, 0.12 ± 0.017, and 0.10 ± 0.018 for $L = 5,13,21,29$, and 39. The reason is that when there is a long-range spatial correlation, regions consisting of dense obstacles are ubiquitous through the force medium. In this situation, the rod will spend a larger time in these islands before it finds a way out through a diffusive channel. In contrast, when the medium posses anticorrelation, the probability of finding a large area having a high local density of obstacles is not large and the medium has a more homogeneous structure. This makes the diffusion more easier comparing to a correlated medium. To see the dependence of the exponent δ on the Hurst exponent H we

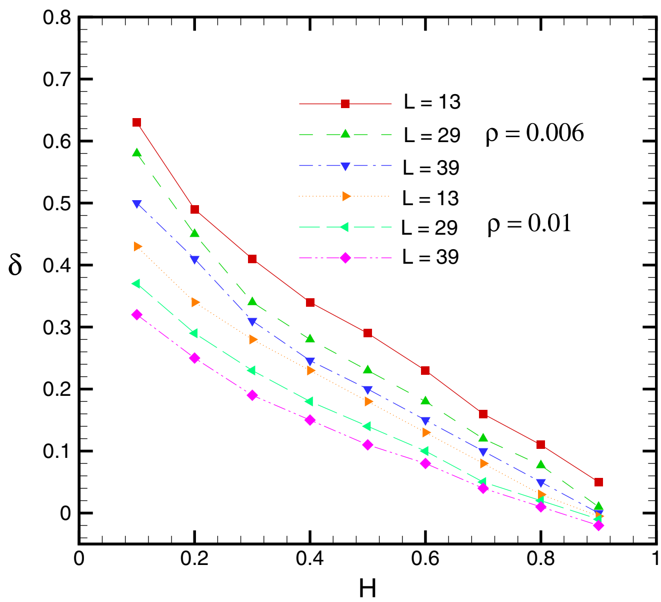

FIG. 6. (Color online) Dependence of diffusion scaling exponent δ on the Hurst exponent H for two media of obstacle densities $\rho = 0.006$ and $\rho = 0.01$.

have performed extensive simulations for various rod lengths. Figure 6 exhibits the results.

You see that δ decreases almost in linear manner with increasing the Hurst exponent H. The physical explanation have been already given in the above lines. To see the effect of obstacles density on rod's motion, we performed extensive simulations for denser media. In Fig. 7 the dependence of exponent δ on obstacles density ρ is shown for the range [0.006,0.05]. The smallest relative standard deviation of the data points is 0.08 whereas the largest one is 0.12.

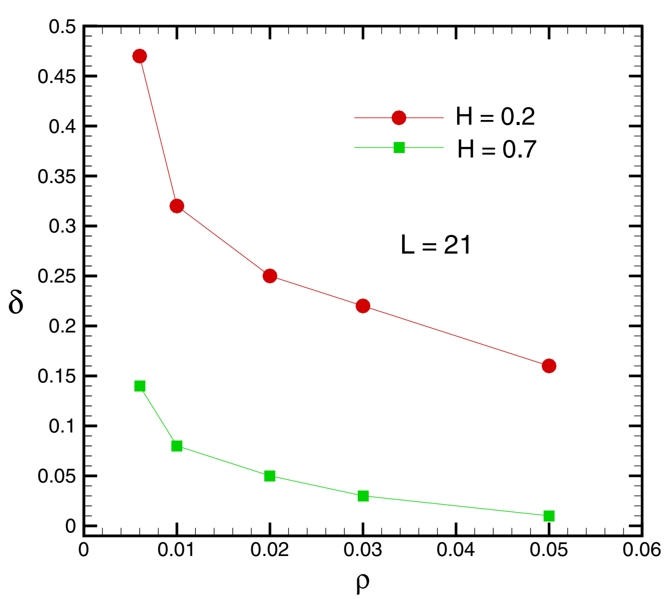

FIG. 7. (Color online) Dependence of diffusion scaling exponent δ on the obstacles density for a medium characterized by ρ for $H = 0.2$.

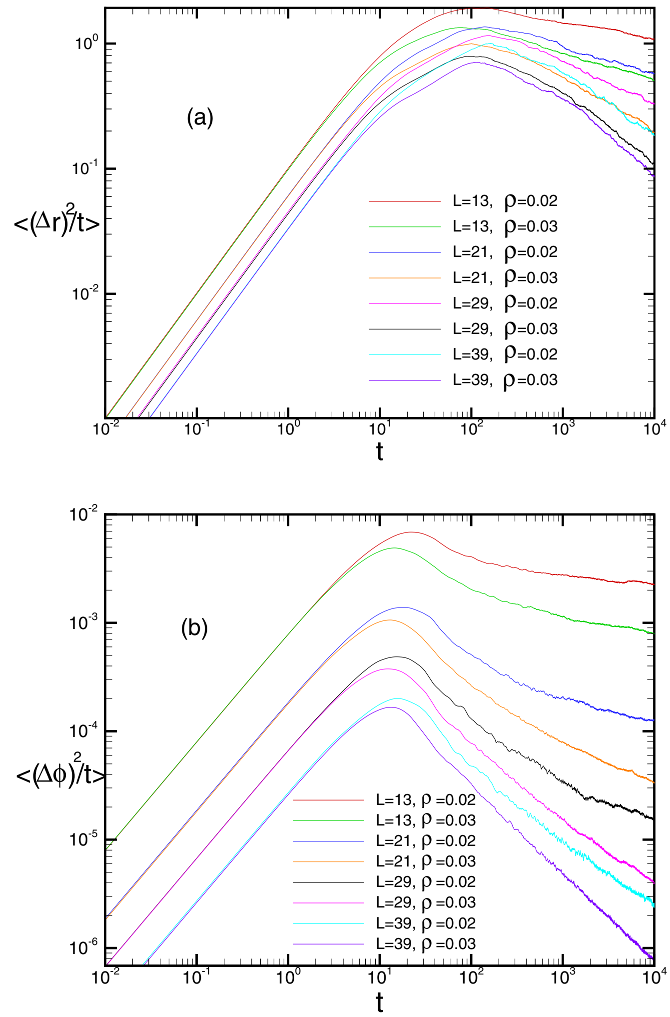

FIG. 8. (Color online) (a) Mean-squared displacement of CM, and (b) angular mean-squared displacement in an uncorrelated media with densities $\rho = 0.02$ and $\rho = 0.03$.

C. Uncorrelated medium ($H = 0.5$)

Despite our main focus in this paper has been on spatially correlated force medium, it would be illustrative to revisit some results for an uncorrelated medium in which the obstacles are distributed randomly through the space. To distinguish our results with the existing ones in the literature, we have considered a denser medium with respect to the one explored in Refs. [19–21]. Figure 8 exhibits the angular as well as position MSD for an uncorrelated medium for densities $\rho = 0.02$ and $\rho = 0.03$. You see that when the density is high (relative to $\rho = 0.006$ considered in Refs. [19,20]) the positional MSD becomes subdiffusive. This is in contrast to normal behavior observed for a medium with $\rho = 0.006$. From rotational viewpoint, for a dense medium the angular MSD becomes subdiffusive as well. The reason is that when the medium becomes denser the obstacles prevent the rod to rotate. This gives to a subdiffusive in angular degree of freedom.

IV. SUMMARY AND CONCLUDING REMARKS

We have investigated the diffusion characteristics of a rigid rodlike object immersed in a two-dimensional random force medium by molecular dynamics. The scattered static pointlike sources of force interact with the rod, which is modeled as an array of aligned points, via a repulsive soft potential. The inhomogeneous spatial distribution of force centers has long-range correlation characterized Hurst exponents greater or less than 0.5. We have investigated the statistical properties of translational and rotational degrees of freedom for various degrees of spatial correlation in the force medium. In particular, the time-averaged mean-squared displacement of the rod's center of mass and its rotational diffusion is obtained for some global densities of force sources. By contrast to uncorrelated distribution of points, the existence of long-range correlation crucially affects the transport characteristics. Our findings demonstrate that the diffusion nature of the rod's CM undergoes a substantial change into a subdiffusive character. We have obtained the diffusion scaling exponent for both correlated and anticorrelated media. Our results show that diffusion in a long-range correlated medium is more slowed down compared to the anticorrelated medium. This is due to existence of large patches with local high density of force source among which the rod is entangled and confined.

ACKNOWLEDGMENTS

We wish to acknowledge the Institute of Advanced Studies in Basic Sciences (IASBS), the Physics Department of Osnabrueck University and in particular Susanne Hahne, and the Grid Computing Group of the Institute for Research in Fundamental Sciences (IPM) for proving us with the computational facilities. Final computational stages of the work were supported by the IPM School of Computer Science. We greatly appreciate this support and in particular Armin Ahmadzadeh. We wish to express our gratitude to Professor Mohammad Sahimi, Reza Jafari from Shahid Beheshti Universty, Mehdi Vaaez Alaaie from Tehran University, and Ali Hamzehpour from Khajeh Nasir University for fruitful discussions. We are indebted to Ehsaan Nedaee from IASBS for providing us with fBm code and enlightening discussions. Useful discussion with Soltaan Abdol Hossein is appreciated.

[1] M. Sahimi, *Heterogenous Material II: Nonlinear and Breakdown Properties of Atomic Modeling* (Springer, Berlin, 2003).
[2] Kurt Binder and Walter Kob, *Glassy Materials and Disordered Solids* (World Scientific, Singapore, 2011).
[3] M. Sahimi, Rev. Mod. Phys. **65**, 1393 (1993); Phys. Rep. **306**, 213 (1998).
[4] *Fractals and Disordered Systems*, edited by A. Bunde and S. Havlin, 2nd ed. (Springer, Berlin, 1996).
[5] B. D. Hughes, *Random Walks and Random Environments* (Oxford University Press, Oxford, 1995).
[6] H. A. Lorentz, Arch. Neerl. **10**, 336 (1905).
[7] F. Höfling, T. Franosch, and E. Frey, Phys. Rev. Lett. **96**, 165901 (2006).
[8] W. Götze, E. Leutheusser, and S. Yip, Phys. Rev. A **23**, 2634 (1981).
[9] T. Keyes, Phys. Rev. A **28**, 2584 (1983).
[10] M. P. Allen, D. Frenkel, and J. Talbot, Computer Phys. Rep. **9**, 301 (1989).
[11] P. G. de Gennes and J. Prost, *The Physics of Liquid Crystals*, 2nd ed. (Oxford University Press, Oxford, 1995).
[12] D. Frenkel and J. F. Maguire, Mol. Phys. **49**, 503 (1983).
[13] A. Chrzanowska and H. Ehrentraut, Phys. Rev. E **66**, 012201 (2002).
[14] P. Pfleiderer, K. Milinkovic, and T. Schilling, Europhys. Lett. **84**, 16003 (2008).
[15] M. Murat and Y. Kantor, Phys. Rev. E **74**, 031124 (2006).
[16] M. E. Foulaadvand and M. Yarifard, Eur. Phys. J. E **34**, 41 (2011).
[17] M. E. Foulaadvand and M. Yarifard, Phys. Rev. E **88**, 052504 (2013).
[18] M. E. Foulaadvand and M. M. Shafiee, Europhys. Lett. **104**, 30002 (2013).
[19] A. J. Moreno and W. Kob, Philosophical Magazine **84**, 1383 (2004).
[20] A. J. Moreno and W. Kob, J. Chem. Phys. **121**, 380 (2004).
[21] A. J. Moreno and W. Kob, Europhys. Lett. **67**, 820 (2004).
[22] A. J. Moreno and W. Kob, AIP Conf. Proc. **708**, 576 (2004).
[23] W. Kob and H. C. Andersen, Phys. Rev. E **51**, 4626 (1995).
[24] S. Mossa, R. DiLeonardo, G. Ruocco, and M. Sampoli, Phys. Rev. E **62**, 612 (2000).
[25] D. Caprion and H. R. Schober, Phys. Rev. B **62**, 3709 (2000).
[26] J. Colmenero, F. Alvarez, and A. Arbe, Phys. Rev. E **65**, 041804 (2002).
[27] W. van Megen, J. Phys.: Condens. Matter **14**, 7699 (2002).
[28] E. R. Weeks and D. A. Weitz, Chem. Phys. **284**, 361 (2002).
[29] A. M. Puertas, M. Fuchs, and M. E. Cates, Phys. Rev. E **67**, 031406 (2003).
[30] M. P. Letinga, E. Barry, and Z. Dogic, Europhys. Lett. **71**, 692 (2005).
[31] M. P. B. van Bruggen, H. N. W. Lekkerkerker, G. Maret, and J. K. G. Dhont, Phys. Rev. E **58**, 7668 (1998).
[32] M. F. Miri, Z. Sadjadi, and M. E. Fouladvand, Phys. Rev. E **73**, 031115 (2006).
[33] M. E. Foulaadvand, A. B. Kolomeisky, and H. Teymouri, Phys. Rev. E **78**, 061116 (2008).
[34] M. Saadatfar and M. Sahimi, Phys. Rev. E **65**, 036116 (2002).
[35] H. Hamzehpour and M. Sahimi, Phys. Rev. E **73**, 056121 (2006).